Hindawi
Advances in Materials Science and Engineering
Volume 2018, Article ID 8150791, 12 pages
https://doi.org/10.1155/2018/8150791

Research Article

Preparation of a Self-Lubricating Cu/h-BN Coating on Cemented Carbide

Tongkun Cao, Zhibin Zhu, and Yajun Liu

College of Electromechanical Engineering, Qingdao University of Science and Technology, Qingdao 266061, Shandong, China

Correspondence should be addressed to Tongkun Cao; caotk@163.com

Received 23 June 2018; Revised 4 November 2018; Accepted 11 November 2018; Published 6 December 2018

Academic Editor: Massimiliano Barletta

In this work, a Cu/h-BN self-lubricating coating was prepared on cemented carbide by electrospark deposition (ESD). The microstructure and properties of the coating were examined. The results showed that no decomposition of or reactions with h-BN occurred. As the h-BN content and capacitance increased, the number of pores and microcracks in the coatings increased. Additionally, as the capacitance increased, the electrode mass loss increased. However, the specimen mass increased first and then decreased. The coating thickness was affected by the capacitance, deposition time, and volume ratio of h-BN to Cu. The results exhibited were consistent over the tests. The self-lubricating coating exhibited excellent tribological behavior under the test conditions, and the worn surface showed features consistent with shear slippage and abrasive wear.

1. Introduction

Cemented carbides are composed of tungsten carbide grains as the aggregate and a ductile metal binder matrix such as cobalt or nickel. Cemented carbides have been widely used in turning tools, molds, and mineral applications because of their high hardness, high toughness, high thermal conductivity, low coefficient of thermal expansion, high thermal shock resistance, and good wear resistance [1–5]. Carbide is more expensive per unit mass than other typical tooling materials and steel. Therefore, to justify this investment, it is necessary for the tool to have a long life. Heavy wear can lead to machinery failure, meaning that many engineering components require high wear properties compared to the substrate material to meet demanding operating environments [6]. One approach to improving the wear properties of a surface involves self-lubricating coatings [7, 8]. Self-lubrication is the process of becoming lubricated without external factors. Self-lubricating coating is usually fabricated by soft metal and solid lubricants, which have low shear strength. The friction coefficient is proportional to the critical shear stress at the interface [9]. When there is a self-lubricating coating on the worn surface, the load is borne by the substrate and the friction is dominated by the self-lubricating coating. Since the shear strength of the self-lubricating coating is much smaller than that of the substrate, the friction coefficient can be reduced. So, self-lubricating coatings can provide lubrication and reduce friction without any external lubrications.

Solid self-lubricating coatings are mainly employed to control friction and wear, especially under harsh application conditions, such as aerospace, high vacuum, high speeds, high pressure, and very low or high temperatures [10, 11]. Under extreme conditions, conventional lubricants cannot provide the desired performance or durability, and in some cases, they cannot be used. At present, PVD (physical vapor deposition) [12, 13] and CVD (chemical vapor deposition) [14] are the most popular and familiar surface technologies to fabricate solid self-lubricating coatings. Additionally, significant attention has been paid to thermal spraying [15] and laser cladding [7, 16] in recent years. However, there is no low-cost preparation method to achieve thick coatings with a strong bonding strength that exhibit good self-lubricating performance. Electrospark deposition (ESD) has some distinct advantages, such as minimal damage to the underlying substrate, metallurgical bonding at the interface, no pollution, high energy density, and low cost. When self-lubricating coatings are fabricated by ESD, the coatings will

achieve a strong bonding strength because of the "cold welding" that occurs between coating and substrate. For soft metals, as matrix will envelope solid lubricants, soft metals and solid lubricants can cooperate with each other to increase the tribology and wear performance. Thus, ESD can be used to achieve thick coatings with a strong bonding strength and good self-lubricating performance in a convenient and cheaper way. However, ESD coating technology has presently focused on coatings such as Ti6Al4V [17] and TiC [18], instead of self-lubricating coatings.

Hexagonal BN is a well-known solid lubricant [19]. Hexagonal BN has a lamellar crystalline structure similar to graphite and MoS_2. However, hexagonal BN has been considered less effective than other solid lubricants, with the exception for high-temperature applications. Hexagonal BN shows remarkable chemical and thermal stability. For example, h-BN is resistant to breakdown at temperatures up to 1000°C in air, 1400°C in vacuum, and 2800°C in an inert atmosphere. Therefore, h-BN is a good lubricant at high temperatures (up to 900°C, even in an oxidizing atmosphere). Some studies have been focused on h-BN-based self-lubricating coatings. Ni60-hBN self-lubricating coatings [20] have been prepared by laser cladding. Under dry sliding conditions, these coatings exhibited excellent wear resistance compared to a Ti6Al4V alloy at relatively high temperatures (300°C and 600°C). A Co-BN (h) nanocomposite coating was prepared using conventional electrodeposition [21]. The results showed that Co-BN (h) nanocomposite coatings exhibited a higher hardness and a lower friction coefficient for the same conditions.

Copper is a soft, malleable, and ductile metal with very high thermal and electrical conductivity [22]. Copper is also a lubricant due to its low shear strength. Along with the self-lubricating properties of graphite, MoS_2, etc., copper self-lubricating composites have been widely used in many industrial applications, such as in brushes, contact strips, and bearing materials [22, 23]. Additionally, copper has been used in a self-lubricating coating as a matrix [24].

In our previous work [9, 25, 26], Cu/h-BN and Cu/Cu-MoS_2 self-lubricating coatings were prepared on steel and high-speed steel, respectively, by ESD. The production process, microstructure, and tribological behaviors of the self-lubricating coatings have been preliminarily investigated, with the results showing that the self-lubricating coatings could reduce the friction coefficient and wear loss. However, cemented carbide is still not used as a substrate for preparing self-lubricating coatings by ESD. Additionally, compared with the Cu/h-BN coating prepared in [9], a different production method was used. Moreover, more self-lubricating coatings should be prepared by ESD and in-depth studies should be carried out on these coatings.

In this paper, a Cu/h-BN self-lubricating coating was prepared on cemented carbide by ESD. The microstructure of the coating was studied. Additionally, this paper focused on the effects that the capacitance, deposition time, and/or the volume ratio of the h-BN to the Cu had on the coating thickness, friction properties, and the electrode's and specimen's mass variations. Also, wear mechanism was discussed.

2. Experiment

2.1. Materials and Procedures. Cemented carbide YT15 (15% TiC and 6%Co, Zhuzhou Cemented Carbide Group Co., LTD, China) was used as the substrate material with the dimensions of 12 × 12 × 4 mm. Prior to deposition, acetone with a concentration of 99.5% was used to clean the substrate surface and the electrode to remove any oil. These were then washed with anhydrous ethanol and dried by hot air.

Five copper pipes filled with h-BN solid lubricant were bound together as the electrode. Figure 1 shows the schematic diagram of the electrode. The purity of copper was greater than 98%, and the average particle size of the h-BN was approximately 1 μm with a purity greater than 99%. The area ratio of h-BN to copper on the electrode cross section represented the volume ratio of h-BN to Cu. When the outer diameters of the copper pipes were Φ1.6, Φ1.8, Φ2.0, Φ2.2, or Φ2.5, the volume ratios (area ratios) of h-BN to copper were 6.7%, 12.5%, 19%, 26%, or 37%, respectively. All the h-BN powder supplied into the electrode is transferred onto the substrate with the molten copper as a result of the electrode vibrating effect during the process, meaning that the volume ratio of h-BN to Cu in the electrode is equal to the volume ratio in the coating.

An ESD machine (model D91350, made in China) was employed during the deposition process with 6 grades of capacitance (80–160–240–320–400–480 μF) and a vibration electrode. The deposition of the Cu/h-BN coating was conducted in multiple consecutive passes in the atmosphere. The movement of the electrode is shown in Figure 2. Two movement paths were used alternately for multiple consecutive passes during the deposition process. The duration of the deposition process was from 5 to 15 minutes. During the experiments, the pulse parameters were as follows: capacitance from the 1st grade to the 6th grade (from 80 to 480 μF), an output voltage of 75 V, and a frequency at 400 Hz.

The coating thickness was measured by a TT260 coating thickness meter (made in China). Six repeated tests were performed for each coating at different positions, and the data reported in this article were the averaged results of these six repeated tests.

2.2. Friction and Wear Testing. Just discussed in introduction, Cu/h-BN and Cu/Cu-MoS_2 self-lubricating coatings were prepared on steel and high-speed steel, respectively, by ESD in our previous works. In this paper, we used the same methods for friction and wear testing. We followed the methods of Cao et al. [25]. The details are as follows.

An SFT-2M ball-on-disc tribometer (Jinan Shidai Shijin Testing Machine Group Co., LTD, China) was employed in friction and wear testing. The diameter of the ball specimen is Φ3 mm, which was made of alloy steel (GCr15: 0.95~1.05%C, 0.2~0.4%Mn, 0.15~0.35%Si, and 1.3~1.65% Cr) with a hardness of HRC60. All the tests were carried out at the temperature of 20°C. The disk specimens were made of the coated YT15. The ball surface was polished to obtain a

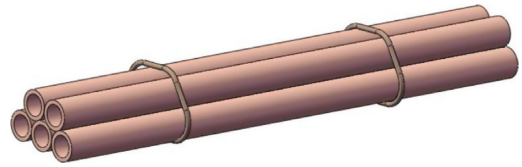

Figure 1: Schematic diagram of the electrode.

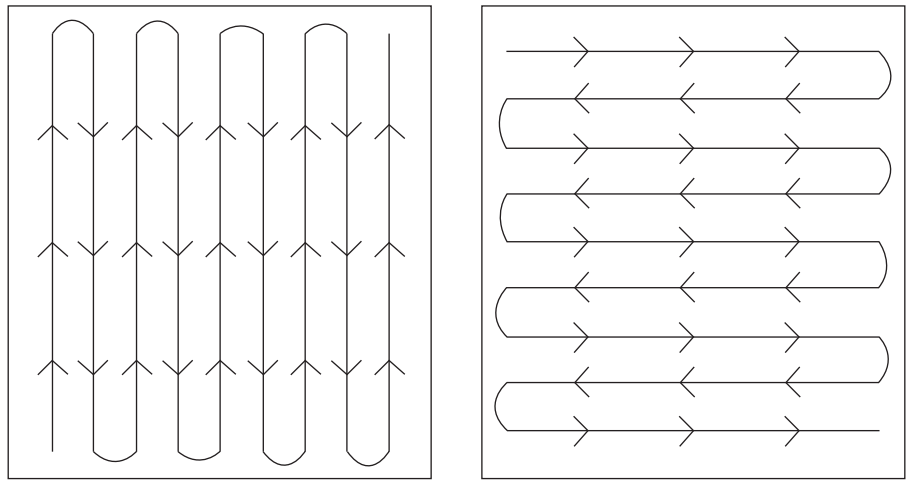

Figure 2: Schematic diagram of the electrode movement.

final surface roughness of Ra = 0.1 μm. The balls and plates were washed with hexane, and then ultrasonically cleaned in fresh hexane and acetone sequentially. The alloy steel ball was fixed, while the coated YT15 disk was rotated. The normal load was 5 N, rotation radius was 4 mm, and rotational speed was 400 r/min. Each test was conducted for the duration of 20 minutes. The friction and wear tests were repeated 3 times for each condition, and the averaged results were used in this article. The friction coefficient was recorded robotically by the tribometer. Wear weight loss was weighed by an electronic balance (minimum 0.1 mg). A scanning electron microscope was employed to obtain the images of the microstructures and the worn regions of the coating.

3. Results and Discussion

3.1. XRD Analysis and Spark Phenomena during the ESD Process. A phenomenon was observed during electrospark deposition. At the beginning of the deposition process, electric discharges between electrodes and substrate were very powerful, and large sparks were observed and splashed far away. With further preparation of the coatings, the spark discharge phenomenon weakened bit by bit. After a Cu layer had covered the substrate surface, the splashing sparking reached a stable stage. There may be 3 reasons for the changes in the splashing spark and discharge status. First, the discharge occurred between the copper electrode and YT15 substrate at the beginning of deposition. This will produce bigger sparking due to the polarity effect of electric spark discharge. During the stable sparking stage, a thin copper layer was already deposited, and sparking discharge occurred between copper and copper. Therefore, the polarity effect of the electric sparking weakened. Second, with the deposition of copper on the substrate surface, the h-BN powder would also be deposited on the substrate surface and mixed with the copper. h-BN is an insulating material, meaning it weakened the electric discharge. Finally, as the coating was built up, the contact area between the electrode and the substrate also increased, which resulted in an overall current density reduction [27]. As a result of all these factors, the spark discharge phenomenon was weakened.

Figure 3(a) shows the X-ray diffraction patterns of Cu/h-BN coating. The results from the XRD indicate that the major phase constituents of the self-lubricating coating are BN, Cu, TiC, and WC. No reactions occurred between these elements and other substances during the ESD process. Figure 3(b) shows an SEM image and EDS spectrum of the Cu/h-BN coating with B, N, Cu, W, C, and Ti elements in the coating. This result further confirms those in the X-ray diffraction patterns. As discussed in Introduction, hexagonal BN has outstanding chemical and thermal stability. In fact, there was no decomposition or reactions of the h-BN. TiC and WC are the main materials of the substrate, meaning that the substrate materials were transferred into the coating by diffusion and splashing effects during the preparation process.

Figure 3(c) shows the EDX analysis results of the area of A, and the element's distribution of N and Cu is shown. As can be seen from Figure 3(c), N and Cu elements are quite uniformly distributed throughout the coating. This indicates that the h-BN phase is uniformly distributed with copper

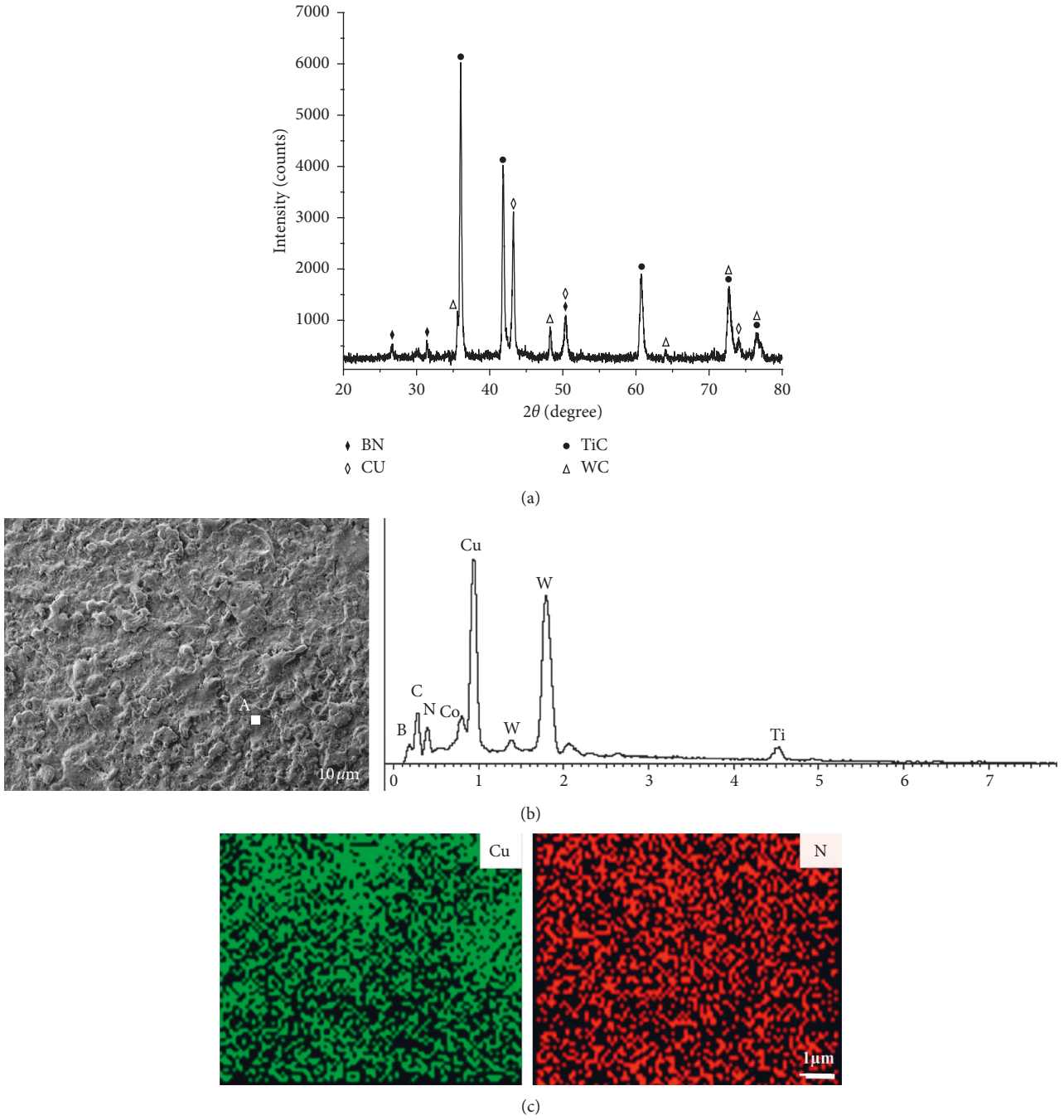

Figure 3: (a) X-ray diffraction patterns; (b) SEM image and EDS spectrum of the Cu/h-BN coating; (c) N and Cu elements distribution corresponding to area A of (b).

and the second phase aggregates are very few. The results are similar with that of the h-BN/Cu coating prepared on AISI 1045 steel [9]. This means that whether the coating is prepared on AISI 1045 steel or YT15 cemented carbide, and coating with uniform distribution of elements can be achieved under the test condition.

3.2. Microstructure of Self-Lubricating Coating. Figure 4(a) shows the SEM images of the coating cross section. There is no clear boundary between the coating and the substrate. The coating is not flat but contains some convex and concave features on the surface. Figure 4(b) shows the SEM micrograph of the coating after etching with 98% vol sulfuric acid. The coating thickness is approximately 50 μm. In our previous work, we verified that there was severe elemental diffusion between coating and substrate during deposition [25], as ESD is a microarc welding process. Therefore, the metallurgical combination will result in a high bonding strength between the coating and the substrate.

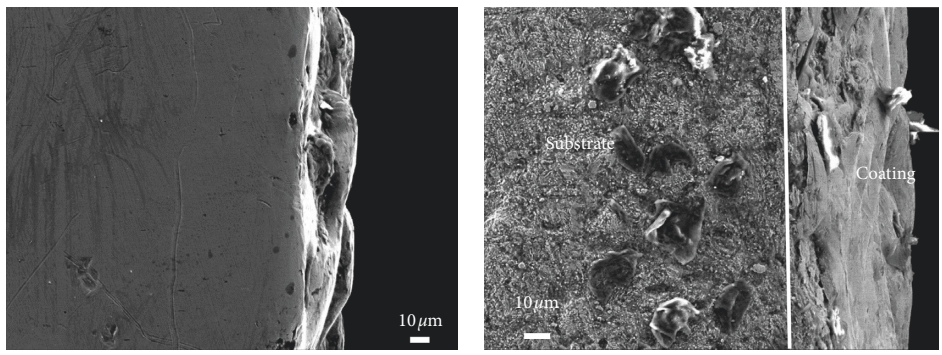

Figure 4: (a) SEM images of the coating cross section and (b) after etching with 98%.vol sulfuric acid.

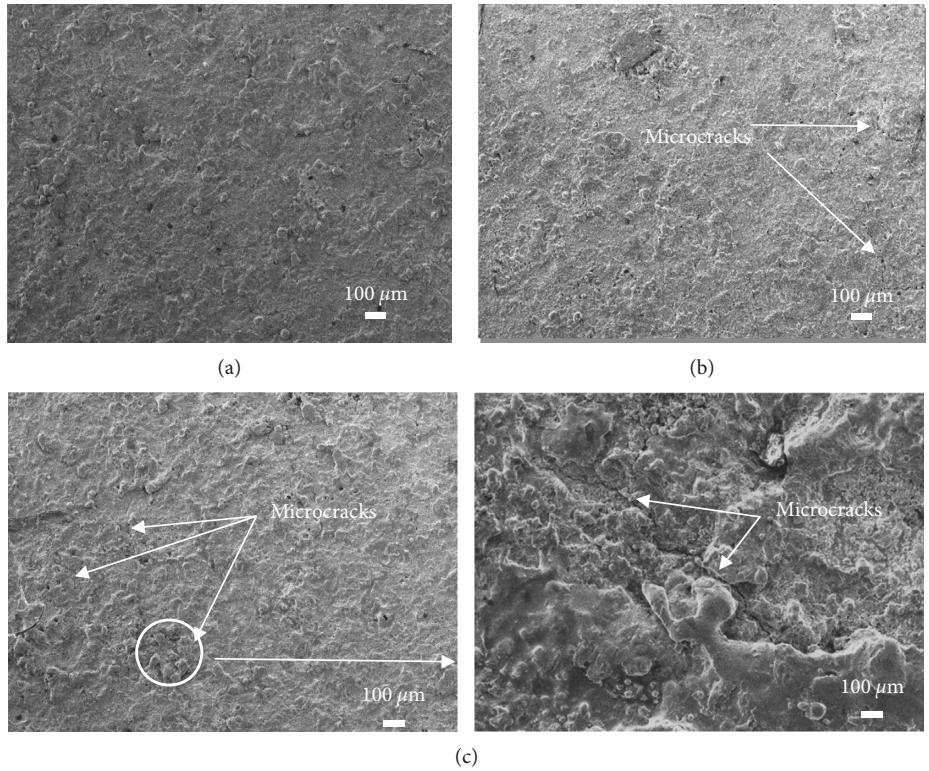

Figure 5: Microstructure of the coating with different volume ratios of h-BN to Cu. (a) 12.5%. (b) 26%. (c) 37%.

Figure 5 shows the typical microstructures of the self-lubricating coating (the capacitance is 3rd grade, and preparation time is 15 minutes). From an examination of the surface characteristics, it is observed that the coating surface had distinct ESD characteristics, such as melted drops, varying size craters, pores, and microcracks, resulting in an uneven surface profile. Figure 5(a) shows the best surface quality with fewer pores and no obvious cracks. As the h-BN content increased, the surface did not change significantly, except that the number of pores and cracks in the coatings were increased. Figure 5(c) shows that when the volume ratio of h-BN to Cu increased to 37%, the coating surface exhibited a large number of cracks. This is mainly because as the volume ratio of h-BN to Cu increased, the strength of the coating decreased. Thus, cracks were generated easily on the coating surface from thermal stress.

Figures 6(a) and 6(b) show the surface microstructure of self-lubricating coating prepared under the 1st grade and 5th grade capacitances, respectively (the volume ratio of h-BN to Cu is 26%). From Figures 5(b) and 6, we see that the coating is roughest when prepared under the 1st capacitance. Compared with Figures 5(b) and 6(a), Figure 6(b) shows that the coating exhibited more pores and microcracks when the coating was prepared under the 5th grade capacitance.

There is a smaller release of energy during the 1st grade capacitance than for the other capacitance grades. Therefore, smaller pieces of metal were melted and dropped onto the

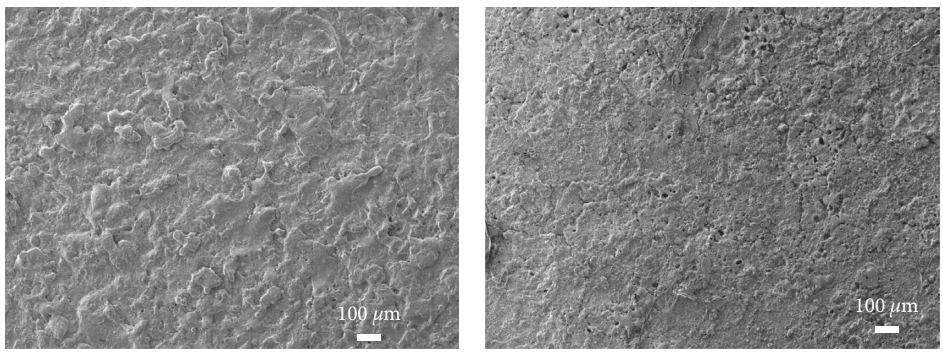

(a) (b)

Figure 6: Microstructure of the coating under different capacitances. (a) 1st grade. (b) 5th grade.

substrate surface. However, the melted metal drops will soon solidify due to the short discharge time, the excellent thermal conductivity of the substrate, and effect of air cooling. During this process, little melted metal splashed away. As a result, the solidified drops on the surface were high and the coating surface was rough. However, bigger pieces of metal were melted and dropped on the substrate surface when the capacitance was either 3rd or 5th grade. Bigger melted metal drops were difficult to solidify in a short time. Therefore, the drops spread over the substrate as a result of the splash force and gravity, causing a more smooth coating. Moreover, more gas was generated and trapped in the drops during the ESD process for greater discharge energies. This led more pores in the coating. As the capacitance increased, higher heat shocks led to more microcracks. In summary, the overall surface quality of the coating was best when prepared using the 3rd grade capacitance. However, the capacitance effect on the coating surface roughness is different than the results in our previous work [26]. Under certain test conditions, the amount of melted metal is different for different electrodes and substrate materials. Additionally, when the melted material is the same, the size of the solidified drops depends on the thermal conductivity of the substrate if the other conditions remain unchanged. These differences led to irregularities in the two works.

3.3. Effect of Capacitance on the Electrode and Specimen Weight Variations

3.3.1. Effect of Capacitance on the Electrode Weight Variation. Figure 7 illustrates the effect of capacitance on the electrode and specimen weight variations. It is indicated that the decrease in electrode weight accelerated with an increase in the capacitance, with the exception of the 1st grade. The reduction in electrode weight reached a maximum under the 6th grade capacitance and was at a minimum under the 2nd grade capacitance. Discharge energy increased within the capacitance. Therefore, the melted material of the electrode increased, and splashing-away materials also increased. The discharge energy for the 6th grade capacitance was the largest, and the correspondingly reduction in the electrode material was also the largest under the 6th grade capacitance.

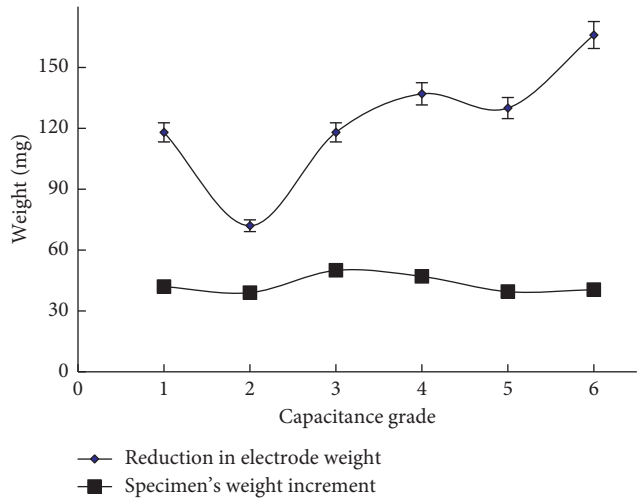

Figure 7: Effect of capacitance on the electrode and the specimen's weight variation (the volume ratio of h-BN to Cu is 19%, and deposition time is 15 min).

In fact, some splashing-away materials were reflected to the electrode's surface because of the small clearance between electrode and coating surfaces. The weight reduction of the electrode was affected by the splashing-away materials and reflected materials. When the capacitance is large, the splashing-away materials dominated the results. However, when the capacitance is small, the reflected materials obviously affected the results. Therefore, the decrease in the electrode material under the 1st grade capacitance was greater than under the 2nd grade capacitance.

3.3.2. Effect of Capacitance on the Specimen Weight Variation. Figure 7 shows that when the capacitance grade was under 3, the specimen's weight increment increased overall with the capacitance grade. However, the specimen's weight increase for grade 2 was less than that of grade 1, although they were close. With further increases in the capacitance grade, the increases to the specimen's weight tapered off. Specimen's weight variation is caused by two factors. One is the quality of the deposited material and the other is the splashing-away quality of the substrate material.

During deposition, a part of the substrate material will splash away. Additionally, the melted electrode material was not deposited completely on the surface of the substrate. There was also a part of melted electrode material splashing away. Therefore, the specimen's weight variation and its trend did not correspond with those of the electrode.

3.4. Thickness of the Coating

3.4.1. Effect of the Capacitance on the Coating Thickness. Figure 8 shows the effects of capacitance on the coating thickness. When the capacitance grade was under 4, the coating thickness increased with the capacitance grade overall. With further increases in the capacitance grade, the coating thickness decreased. During electrospark deposition, when material removal was less than the transferred amount of electrode material to the substrate, the coating thickness exhibited an upward trend and vice versa.

These results are because that melted electrode materials increased with the capacitance and the discharge energy. As a result, the deposited material on the substrate surface increased. Therefore, the thickness of the coating increased firstly. With further increases in the capacitance, the splashing effect of the melted drops was also enhanced. As the discharge energy increased, vaporized materials and gas increased, and the splashing-away materials also increased. At the same time, this increases the pores of coating surface, as shown in Figure 6(b). However, the material deposited on the substrate surface decreased. Additionally, as the discharge energy increased, the effect of thermal shock was enhanced, and the stress in the coating increased. Under high capacitance, high stress can result in microcracks as shown in Figure 6(b). Figure 6(b) shows, when coating was prepared under 5th grade capacitance, there are obvious microcracks and more pores on coating surface. These pores and microcracks can cause the coating to peel down easily and can decrease the coating thickness.

3.4.2. Effect of Deposition Time on the Coating Thickness. Figure 9 shows the effect of deposition time on the coating thickness. The maximum coating thickness was 58.5 μm for a deposition time of 10 min. When the deposition time was less or more than 10 min, the coating thickness decreased. The coating thickness was very thin during the initial stage, and more material was deposited on the substrate as the deposition time increased, leading to an increase in the coating thickness. Electrospark deposition coating is composed of numerous deposition points. With further increases in the deposition time, the thermal shock times at every deposition point of the coating also increased. As the deposition time increased, the effect of the thermal shock was enhanced, which can lead to increased thermal stresses in the coating. Finally, fatigue cracks, which are similar to the cracks in Figure 6(b), would be produced in the coating, and broken fragments would be separated from the deposition layer and fall off under the effect of the electric spark explosion and the mechanical force of the electrode. This led to the decrease in the thickness of the coating.

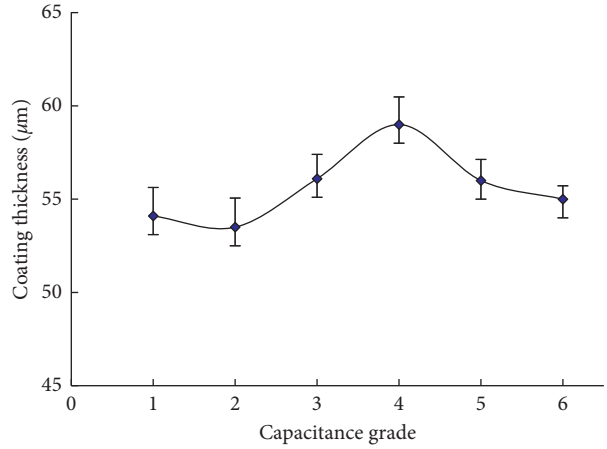

Figure 8: Effect of capacitance on the coating thickness (the pipe diameter of the electrode is Φ2.0, and the deposition time is 15 min).

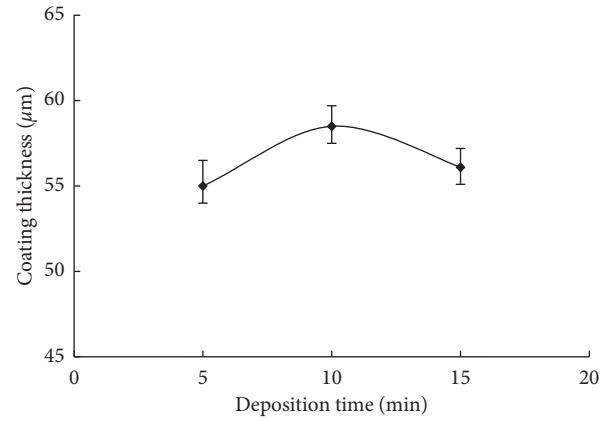

Figure 9: Effect of deposition time on coating thickness (the pipe diameter of the electrode is Φ2.0, and the capacitance is the 3rd grade).

3.4.3. Effect of the Volume Ratio of h-BN to Cu on the Coating Thickness. Figure 10 shows the effect of the volume ratio of h-BN to Cu on the coating thickness. When the ratio of h-BN to Cu was under 19%, the coating thickness exhibited an increasing trend overall as the ratio of h-BN to Cu increased. With further increases in the ratio of h-BN to Cu, the coating thickness decreased. The reason for this is that during the deposition process, the copper pipe constituting the electrode was melted by the electric sparking. However, the h-BN powder filled in the copper pipe was not affected by the electric sparking, as the h-BN is nonconductive and not in the plasma channel. The same conclusion has been drawn in our previous work [25]. The h-BN powder was deposited onto the substrate together with the molten Cu to form a coating. Under certain deposition conditions, the deposition volume of Cu per minute is essentially unchanged. As the volume ratio of h-BN to Cu in the electrode increased, the h-BN volume in the coating will increase. Accordingly, the total coating volume increased. Therefore, the coating thickness increased with the volume ratio of h-BN to Cu. When the h-BN content was high in the coating, the strength

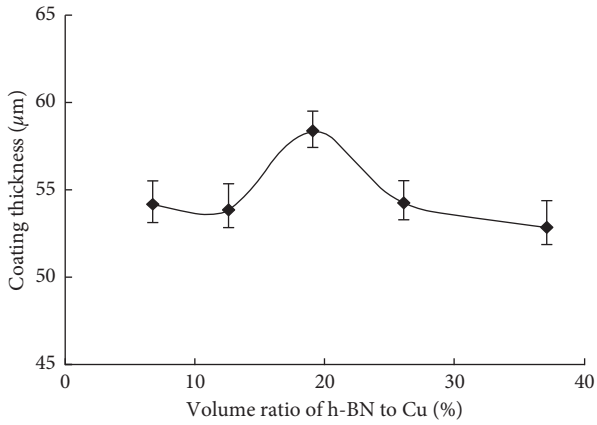

Figure 10: Effect of the volume ratio of h-BN to Cu on coating thickness (capacitance is the 3rd grade, and deposition time is 10 min).

of the coating was low, resulting in cracking and spalling fragments on the coating surface. Moreover, as the h-BN content of the coating increased, the chance of h-BN decomposition also increased during the deposition process. The gas generated by the decomposition could produce more pores in the coating, which could further damage the structure and strength of the coating. As shown in Figure 5, there are fewer pores and no obvious cracks on the coating surface when the volume ratio of h-BN to Cu is 12.5%. When the volume ratio of h-BN to Cu increased to 26%, there are some pores and obvious microcracks on the coating surface. When it is 37%, there are more cracks and pores on the coating surface. Therefore, the coating thickness decreased with further increases in the volume ratio of h-BN to Cu.

From the above discussion, it can be seen that capacitance, deposition time, and volume ratio of h-BN to Cu all have an effect on coating thickness. Under this test condition, the 4th capacitance grade, deposition time of 10 min, and volume ratio of h-BN to Cu of 19% are the optimal parameters for coating thickness. In fact, besides the three factors, there are still some other factors to affect coating thickness, such as substrate material and preparing method. In our previous work [26], the coating thickness can be 100 μm, which was prepared by another method on AISI 45 steel. The coefficient of thermal expansion of AISI 45 steel is closer to copper than YT15. So the thermal stresses of coating prepared on AISI 45 steel is less than that of coating prepared on YT15. This contributes to an increase in the coating thickness.

3.5. Friction and Wear Properties of Coating

3.5.1. Effect of the Capacitance on the Friction and Wear Properties. Figure 11 shows the effect of the capacitance on the friction coefficient and wear weight loss. Figure 11(a) shows that, during the friction running-in stage, the friction coefficient of the self-lubricating coating was unstable. After 5 minutes, the friction entered the stable phase. The friction coefficient showed a slightly decreasing trend with an increase in sliding friction time. From Figure 3(c), copper and h-BN were distributed homogeneously in the coating. Therefore, materials homogeneity is not the main factor to affect friction. However, the flatness of coating can affect friction greatly. As discussed above, the coating surface with distinct ESD characteristics is uneven. So, at the beginning of sliding, friction was not stable. With continuation of sliding, coating surface was planished and the friction coefficient was stable.

It can be seen from Figures 11(a) and 11(b) that the friction coefficient and the wear weight loss of the self-lubricating coating first decreased and then increased with an increase in the capacitance. From Figures 5(b) and 6, for a smaller capacitance, the self-lubricating coating surface was rougher and had no clear microcracks. Therefore, the friction coefficient was larger, but the wear weight loss was smaller when the capacitance was smaller. When the capacitance was increased to the 3rd grade, the surface roughness of the coating decreased, as did the friction coefficient. However, only a few microcracks were generated on the surface, suggesting that the coating's mechanical properties would be slightly weakened compared to the coating prepared under 1st grade. Under the combined action of the roughness and mechanical properties, the wear weight loss decreased too. With further increases in capacitance, many cracks and pores were generated on the coating surface. Therefore, the friction coefficient and the wear weight loss both increased. Figure 11(b) shows the wear weight loss of the uncoated substrate was more than that of the 1st grade and 3rd grade capacitances, meaning that the self-lubricating coating has better wear resistance than uncoated cemented carbide. However, the wear weight loss of the 5th grade was more than the uncoated cemented carbide. As discussed, the coating prepared under the 5th grade has many cracks and pores on the coating surface. The cracks and pores led to a higher wear weight loss than the uncoated cemented carbide.

Compare with our previous work [9, 26], the roughness of coating prepared on the AISI 45 steel is bigger than that of coating prepared on the YT15 under the same condition. Electrical conductivity of YT15 is lower than that of AISI 45 steel. Under the same electrical parameters, more electrode material will be transferred to AISI 45 steel. Thermal conductivity of YT15 is also lower than that of AISI 45 steel. Lower thermal conductivity means that molten electrode materials transferred to substrate need more time to solidify. These two mean that there is more time to flow before solidification of molten electrode materials. This can lead to bigger roughness of coating prepared on the AISI 45 steel. On the contrary, this also can lead more pore and microcracks on the coating. So, the friction coefficient and wear loss of the coating prepared on the AISI 45 steel increase with the increase in capacitance. However, the coating prepared on the YT15 showed different trends just as mentioned above.

3.5.2. Effect of the Volume Ratio of h-BN to Cu on the Friction and Wear Properties. Figure 12 shows the effect of the volume ratio of h-BN to Cu on the friction coefficient and wear weight loss. The friction coefficient and wear weight

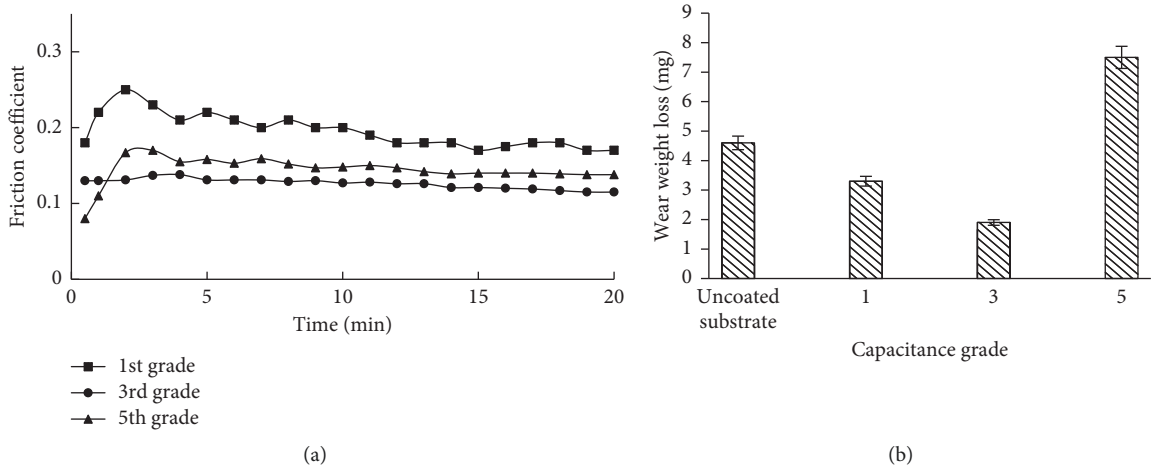

Figure 11: Effect of capacitance on (a) friction coefficient and (b) wear weight loss (pipe diameter of electrode is Φ1.8, and capacitance is the 3rd grade).

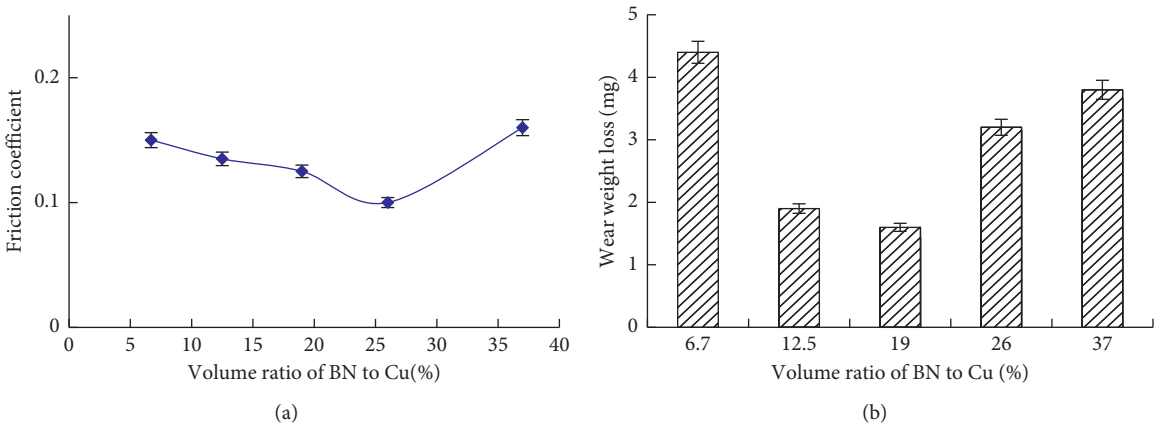

Figure 12: Effect of the volume ratio of h-BN to Cu on (a) friction coefficient and (b) wear weight loss (capacitance is the 3rd grade).

loss of the self-lubricating coating first decreased and then increased with the volume ratio of h-BN to Cu. The friction coefficient was minimized (0.1) when the volume ratio of h-BN to Cu was 26%. The wear volume was minimized at 1.6 mg when the volume ratio of h-BN to Cu was 19%. As the volume ratio of h-BN to Cu increased, the h-BN content in the self-lubricating coating also increased. Therefore, the self-lubricating effect of the coating was enhanced. The wear volume and friction coefficient of the coating decreased with an increase in the volume ratio of h-BN to Cu (up to 26% and 19%, respectively). However, as previously described, the strength of the coating decreased with the increase in the volume ratio of h-BN to Cu and easily resulted in cracks on the coating surface under thermal shock, as shown in Figure 5(c). This easily results in coating spalling, which caused the self-lubricating effect to decrease. Finally, with further increases in the ratio of h-BN to Cu, the friction coefficient and wear weight loss both increased.

3.5.3. Worn Surface. Figure 13 shows a typical worn surface from self-lubricating coatings. Compared with the uneven coating surface, the wear scar was smooth, and craters and convexities were planished. Figure 13(a) shows the worn track and clear boundary between coating and worn track. Figure 13(b) shows the worn track of the coating. As can be seen from Figure 13(b), the worn surface is smooth. There were no obvious peaks, craters, and pores, and there were some obvious traces of shear slippage on the wear scar. From Figure 13(c), there were some scratches on the wear surface, an obvious characteristic of abrasive wear. During the wear process, the coating did not fell off in whole because of the metallurgical combination between the coating and the substrate.

The elements of the worn surface were analyzed by the EDS spectrum. The result showed that the elemental composition of the worn surface was not clearly changed compared with the original coating. However, there were some additional elements from the coating on the worn surface of the ball specimen. Figure 14 shows an SEM image and EDS spectrum of the worn surface of the ball specimen. The SEM image showed that there were some materials squama-like on the worn surface. From the EDS spectrum, there were B, N, Cu, and Ti elements from the Cu/BN coating originally on the worn surface of the ball,

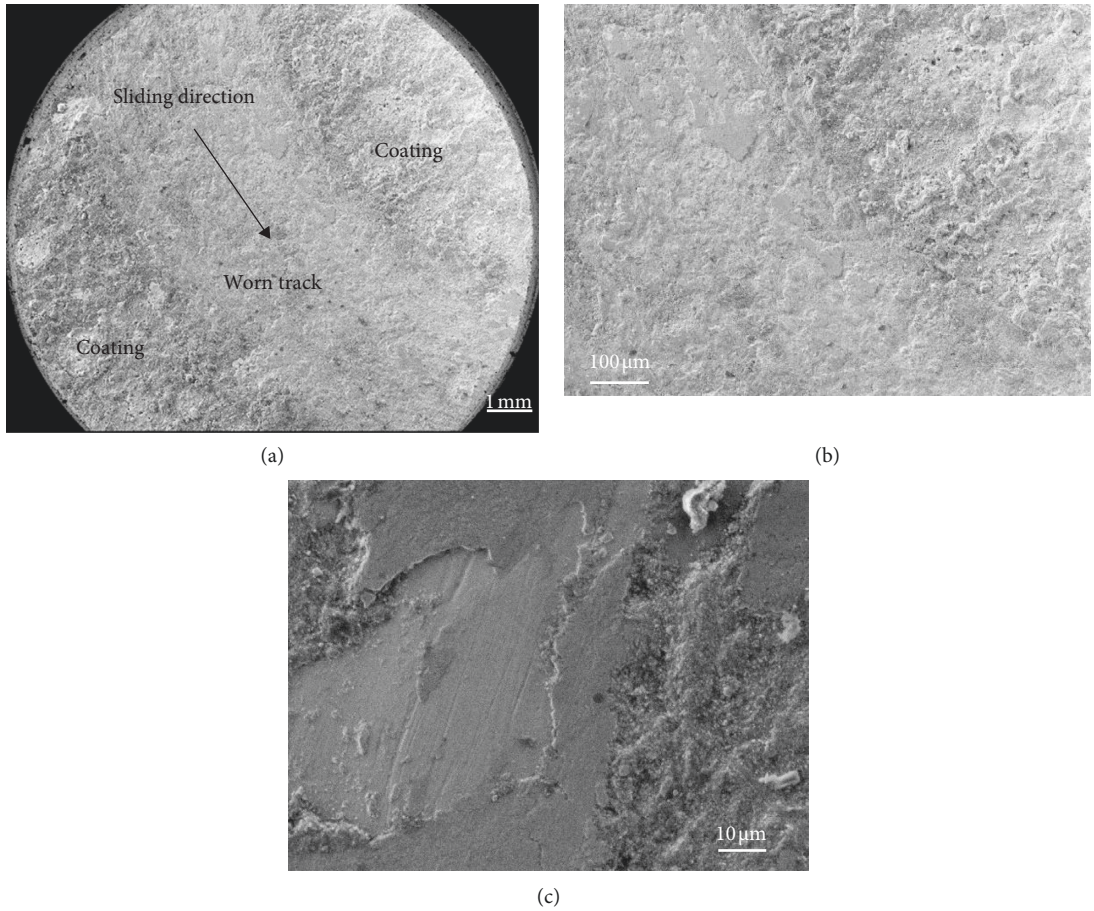

Figure 13: Worn surface (duration of 20 minutes, normal load 5 N, rotation radius 4 mm, and rotational speed 400 r/min).

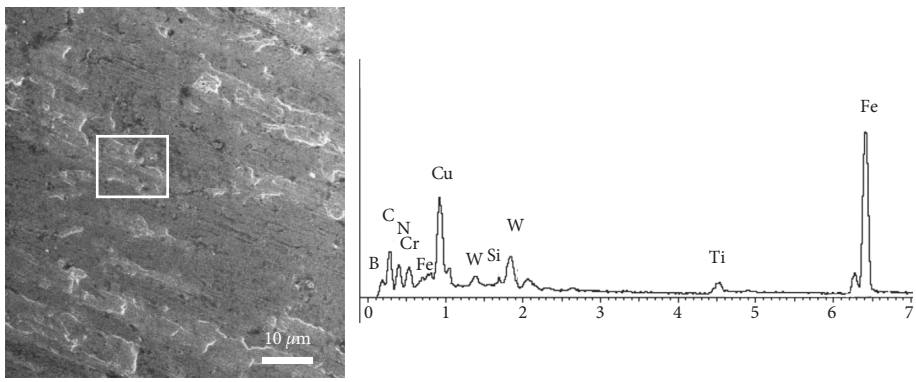

Figure 14: SEM image and EDS spectrum of the worn surface from the ball specimen.

meaning that coating materials transferred to the ball. Thus, friction occurs between the transfer film and the coating, which reduces friction, prevents adhesion, reduces the friction temperature, and reduces wear.

Figure 15 shows the schematic of wear surface evolution. Figure 15(a) shows the state before the beginning. When slide begins, due to the good ductility of copper matrix, the plastic flow of copper will occur under the action of friction force and friction heat, which makes the convex part of the coating surface slide toward the craters, as shown in Figure 15(b). After repeated friction on the friction surface, the convex part of self-lubricating coating is smeared on the wear surface and the craters and pores are filled. Thus the worn surface becomes smooth and some coating material can be transferred to ball surface to form transfer film, as shown in Figure 15(c). Even when part of the surface of coating is destroyed and peeled off to form craters during the wear process, copper and solid lubricants on other surfaces will "flow" to the damaged area, filling the craters. So the local damage can be repaired to a certain extent.

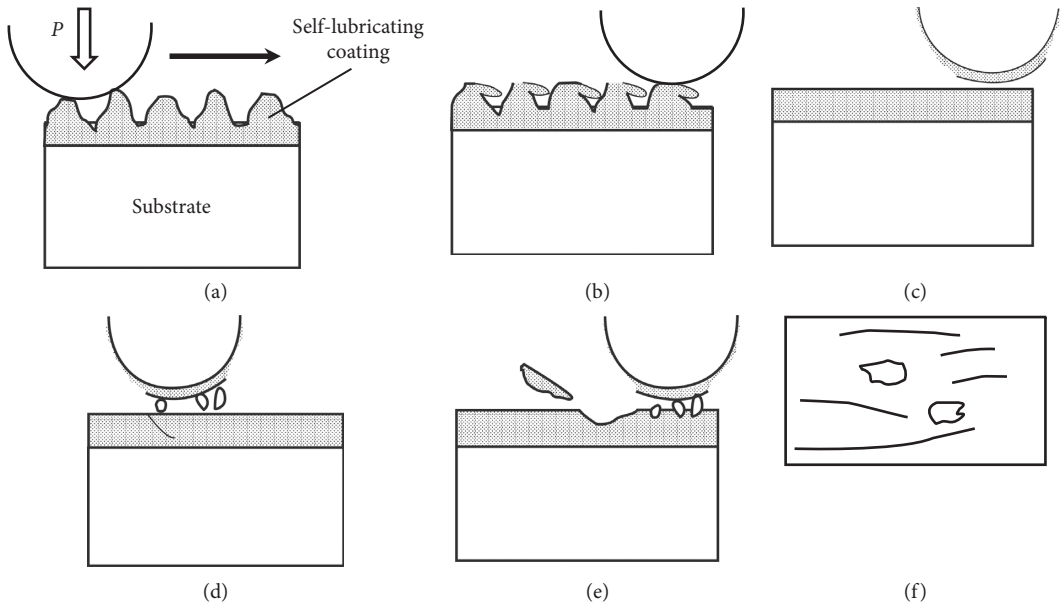

Figure 15: Schematic of wear surface evolution.

With the friction time increase, due to the different thermal expansion coefficients between coating and substrate, friction heat is generated during the friction process, resulting in thermal stress between the coating and the substrate. The coating is also subjected to load and friction force. So with the increase of friction time, the coating will produce fatigue cracks. Moreover, under various stresses, hard particles will fall off from worn surfaces and enter the interface between coating and ball, as shown in Figure 15(d). The cracks are continuously expanded under various stresses, resulting in the damage of the coating. At the same time, under the action of load and friction, the hard particles will penetrate into the coating and cause sculpture damage to the coating, as shown in Figure 15(e). The furrow action of hard particles will increase friction. With the continuous damage of the coating, the whole coating will be destroyed in large area, as shown in Figure 15(f).

4. Conclusions

In this work, Cu/h-BN coatings were fabricated successfully by ESD on cemented carbide. There was a metallurgical combination, which usually has high bonding strength, between the coating and the substrate. The coating has distinct ESD characteristics, and the h-BN content and capacitance affect the coating microstructures. During the deposition process, the lessened electrode material is not completely transferred to the substrate and is obviously affected by the capacitance. The effects that the capacitance, the volume ratio of h-BN to Cu, and the deposition time have on the coating thickness exhibited similar trends: increased first and then decreased. The capacitance and volume ratio of h-BN to Cu had a clear effect on the wear weight loss and friction coefficient. The friction coefficient and the wear weight loss first decreased and then increased with the capacitance and volume ratio of h-BN to Cu. However, the friction coefficient and the wear rate decreased with an increase in the speed. The friction coefficient decreased and the wear rate increased with an increase in the load. The worn surface exhibited obvious traces of shear slippage and characteristics of abrasive wear.

Data Availability

All the data used to support the findings of this study have been deposited in the Google drive repository (https://drive.google.com/file/d/1SRCpA2QA1x6V9EpNCtS3UpOyfac44DFU/view?usp=sharing).

Conflicts of Interest

The authors declare that they have no conflicts of interest.

Acknowledgments

This work was supported by the Shandong Provincial Natural Science Foundation, China (ZR2016EEM41 and ZR2017MEE076).

References

[1] L. Emanuelli, M. Pellizzari, A. Molinari et al., "Thermal fatigue behaviour of WC-20Co and WC-30(CoNiCrFe) cemented carbide," *International Journal of Refractory Metals and Hard Materials*, vol. 60, pp. 118–124, 2016.

[2] A. Marquezherrera, B. Gabriel, E. Hernandezrodriguez et al., "Boride coating on the surface of WC–Co-based cemented carbide," *International Journal of Materials Research*, vol. 107, no. 7, pp. 676–679, 2016.

[3] Y.-I. Chen, Yu-T. Lin, Li-C. Chang, and J.-W. Lee, "Preparation and annealing study of CrTaN coatings on WC-Co," *Surface and Coatings Technology*, vol. 206, no. 7, pp. 1640–1647, 2011.

[4] J. Tang, J. Xiong, Z. Guo et al., "Microstructure and properties of CVD coated on gradient cemented carbide with different WC grain size," *International Journal of Refractory Metals and Hard Materials*, vol. 61, pp. 128–135, 2016.

[5] C. Wang, C. Jiang, and V. Ji, "Thermal stability of residual stresses and work hardening of shot peened tungsten cemented carbide," *Journal of Materials Processing Technology*, vol. 240, pp. 98–103, 2017.

[6] S. W. Huang, M. Samandi, and M. Brandt, "Abrasive wear performance and microstructure of laser clad WC/Ni layers," *Wear*, vol. 256, no. 11-12, pp. 1095–1105, 2004.

[7] X.-B. Liu, X.-J. Meng, H.-Q. Liu et al., "Development and characterization of laser clad high temperature self-lubricating wear resistant composite coatings on Ti–6Al–4V alloy," *Materials and Design*, vol. 55, pp. 404–409, 2014.

[8] D. Z. Segu, J.-H. Kim, Si G. Choi et al., "Application of Taguchi techniques to study friction and wear properties of MoS_2 coatings deposited on laser textured surface," *Surface and Coatings Technology*, vol. 232, pp. 504–514, 2013.

[9] T. Cao and Z. Xiao, "Tribological behaviors of self-lubricating coating prepared by electro-spark deposition," *Tribology Letters*, vol. 56, no. 2, pp. 231–237, 2014.

[10] F. Fernandes, T. Polcar, and A. Cavaleiro, "Tribological properties of self-lubricating TiSiVN coatings at room temperature," *Surface and Coatings Technology*, vol. 267, pp. 8–14, 2015.

[11] Giuseppe Tronci and M. B. Marshall, "Understanding the behaviour of silver as a low friction coating in aerospace fasteners," *Tribology International*, vol. 100, pp. 162–170, 2016.

[12] Y. Wang, J.-W. Lee, and D. Jenq-Gong, "Mechanical strengthening in self-lubricating CrAlN/VN multilayer coatings for improved high-temperature tribological characteristics," *Surface and Coatings Technology*, vol. 303, pp. 12–17, 2016.

[13] Y. Q. Xing, J. X. Deng, X. S. Wang et al., "Effect of laser surface textures combined with multi- solid lubricant coatings on the tribological properties of Al_2O_3/TiC ceramic," *Wear*, vol. 342, pp. 1–12, 2015.

[14] J. Solis, H. Zhao, C. Wang et al., "Tribological performance of an H-DLC coating prepared by PECVD," *Applied Surface Science*, vol. 383, pp. 222–232, 2016.

[15] H. Du, C. Sun, W. Hua et al., "Structure, mechanical and sliding wear properties of WC–Co/MoS_2–Ni coatings by detonation gun spray," *Materials Science and Engineering: A*, vol. 445–446, pp. 122–134, 2007.

[16] X.-L. Lu, X.-B. Liu, P.-C. Yu et al., "Effects of annealing on laser clad Ti_2SC/CrS self-lubricating anti-wear composite coatings on Ti6Al4V alloy: microstructure and tribology," *Tribology International*, vol. 101, pp. 356–363, 2016.

[17] D. Salih, A. S. Levent, and K. Kemal, "Characterization and mechanical properties of the duplex coatings produced on steel by electro-spark deposition and micro-arc oxidation," *Surface and Coatings Technology*, vol. 236, pp. 303–308, 2013.

[18] Yu. G. Tkachenko, D. Z. Yurchenko, V. F. Britun, L. P. Isaeva, and V. T. Varchenko, "Structure and properties of wear-resistant spark-deposited coatings produced with a titanium carbide alloy anode," *Powder Metallurgy and Metal Ceramics*, vol. 52, no. 5-6, pp. 306–313, 2013.

[19] Y. Kimura and T. Wakabayashi, "Boron nitride as a lubricant additive," *Wear*, vol. 232, no. 2, pp. 199–206, 1999.

[20] X.-L. Lu, X.-B. Liu, P.-C. Yu et al., "Synthesis and characterization of Ni60-hBN high temperature self-lubricating anti-wear composite coatings on Ti6Al4V alloy by laser cladding," *Optics and Laser Technology*, vol. 78, pp. 87–94, 2016.

[21] Z. Shahri, S. R. Allahkaram, and A. Zarebidaki, "Co-BN (h) nanocomposite coatings were prepared by means of the conventional electrodeposition," *Applied Surface Science*, vol. 276, pp. 174–181, 2013.

[22] A. G. Kostornov, I. Fushchich, T. M. Chevychelova et al., "Interaction between components of the copper-based self-lubricating antifriction composite at 900 and 950°C," *Powder Metallurgy and Metal Ceramics*, vol. 54, no. 1-2, pp. 16–22, 2015.

[23] H. Akbulut, G. Hatipoglu, H. Algul et al., "Co-deposition of Cu/WC/graphene hybrid nanocomposites produced by electrophoretic deposition," *Surface and Coatings Technology*, vol. 284, pp. 344–352, 2015.

[24] P. J. Kelly, H. Li, P. S. Benson et al., "Comparison of the tribological and antimicrobial properties of CrN/Ag, ZrN/Ag, TiN/Ag, and TiN/Cu nanocomposite coatings," *Surface and Coatings Technology*, vol. 205, no. 5, pp. 1606–1610, 2010.

[25] T. Cao, S. Lei, and M. Zhang, "The friction and wear behavior of Cu/Cu-MoS_2 self-lubricating coating prepared by electrospark deposition," *Surface and Coatings Technology*, vol. 270, pp. 24–32, 2015.

[26] T. Cao and Z. H. Xiao, "Study on self-lubricating coating prepared by electrospark deposition," *Materials Science and Technology*, vol. 31, no. 4, pp. 481–486, 2015.

[27] S. K. Tang, T. C. Nguyen, and Y. Zhou, "Materials transfer in electro-spark deposition of TiC_p/Ni metal-matrix composite coating on Cu substrate," *Welding Journal*, vol. 89, pp. 172–180, 2010.